Notes

On the Conformation of Tiazofurin Analogues

Gergely M. Makara* and György M. Keserû†

Department of Molecular Biology and Pharmacology, Washington University at St. Louis, St. Louis, Missouri 63110, and Department of Chemical Information Technologies, Technical University of Budapest, Szt. Gellert ter 4, H-1521, Budapest, Hungary

Received March 3, 1997[⊗]

Tiazofurin, an important inhibitor of inosine 5′-monophosphate dehydrogenase, has been argued to possess a restricted glycosylic bond due to an energetically favorable intramolecular (1−4) electrostatic interaction between the partial positive sulfur and the negative oxygen of the ribose. This rigidity has been appointed as a plausible cause that leads to activity in the sulfur containing compounds as opposed to the inactive oxazofurin-like analogues *(i.e. S* is replaced by an oxygen) that lack this favorable interaction. We reinvestigated this notion by using computational methods to report that although the above interaction (or its lack) is likely to contribute to the low-energy conformation of these classes of molecules, the flexibility of the glycosylic bond is ultimately determined by steric interaction of the heteroatoms with the C2′-H and O4′ of the ribose. Application of this theory in the design of new analogues is presented as well.

Introduction

Selenazofurin (**1a**, Figure 1) and tiazofurin (**2a**) are *C*-glycosyl nucleosides that have been the subject of numerous studies due to their significant antitumor activity against several cell lines. Biological effects also include ability to induce differentiation in neoplastic cells, downregulation of oncogene activity, and inhibition of G-protein-mediated cellular signaling mechanism. The compounds have been shown to act through inhibition of inosine monophosphate dehydrogenase (IMPD), the penultimate enzyme in the guanine nucleotide biosynthesis.[1] Both tiazofurin and selenazofurin have to be converted to the active forms, the dinucleotides "TAD" and "SAD" in sensitive cells to become NAD^+ analogues that are very effective inhibitors of IMPD and to less extent of some other dehydrogenases as well.[2] Recently a new analogue, thiophenfurin (**3a**), has been reported to retain the full activity of tiazofurin despite the replacement of the nitrogen with a CH moiety.[3]

Substitution of the other heteroatom (S or Se) with oxygen, however, has been proven to abolish all potency, rendering oxazofurin (**4a**) and furanfurin (**5a**) inactive.[3,4] This has been proposed to be the result of the loss of favorable intramolecular contact between heterocyclic S (Se) and the ribose oxygen. The electrostatic attraction between the negatively charged oxygen and the positively charged sulfur (or selenium) has been argued to be the chief cause of constrained rotation around the glycosylic bond which fixes the conformation around that torsional angle.[5] This preorganization into the active conformation may lead to significant entropic and enthalpic gain during binding. The favored conformation of tiazofurin has been found to be retained in the solid state and in enzyme bound form as well.[6,7] The O−O repulsion observed by *ab initio* calculations of model compounds has been appointed to be responsible for the inactivity of **4a** and **5a** due to forcing the glycosylic torsional angle to adopt a different conformation.[3,4]

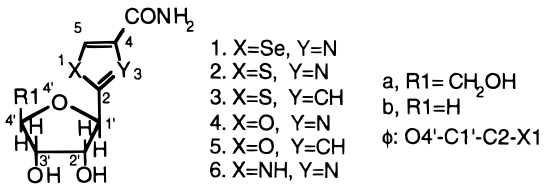

Figure 1. Tiazofurin analogues.

The X-ray structure of IMPD with bound mycophenolic acid, a unique NAD^+ analogue, has recently been reported.[8] The coordinates of the complex have not been deposited to the protein database to date; thus no conclusions can be drawn on the three-dimensional stereospecific interactions in the active site. Mycophenolic acid, tiazofurin, and selenazofurin were shown to bind to the same nicotinamide binding region based on multiple inhibitor experiments.[9] Thus, the recently emerged data on the solid state structure is likely to trigger a renewed interest in tiazofurin analogues as well.

We reexamined the conformational flexibility of **2b**−**5b** using computational methods at the *ab initio,* semiempirical, and molecular mechanics levels. Our calculations which included the full ribose moiety suggest that rotational constraint around the C-glycosylic bond is imposed by unfavorable van der Waals (vdW) contacts between the heteroatoms and the ribose C2′-H and O4′ rather than electrostatic interactions. The latter is expected to give only a minor contribution along with other effects in high dielectric media. A possible exploitation of these findings in the design of new analogues is also demonstrated.

* Author to whom correspondence should be addressed at Washington University at St. Louis.
† Technical University of Budapest.
⊗ Abstract published in *Advance ACS Abstracts,* November 15, 1997.

S0022-2623(97)00129-5 CCC: $14.00

Table 1. Point Charges on Heteroatoms

	3-21G*		6-31G*	
compd	NBO	CHelpG	NBO	CHelpG
2b	S1: 0.54	S1: 0.05	S1: 0.43	S1: −0.02
	N3: −0.55	N3: −0.49	N3: −0.58	N3: −0.47
	O4′: −0.61	O4′: −0.51	O4′: −0.63	O4′: −0.42
4b	O1: −0.53	O1: −0.35	O1: −0.57	O1: −0.28
	N3: −0.53	N3: −0.67	N3: −0.56	N3: −0.63
	O4′: −0.59	O4′: −0.49	O4′: −0.65	O4′: −0.46

Results

Compounds **1a**−**5a** have been subject to *ab initio* and some semiempirical studies on model fragments. *Ab initio* calculations have been carried out with fragments used for **2a** and **4a** where the entire ribose fragment was omitted and modeled by a methoxymethyl group while for **3a** and **5a** only the 4′-hydroxymethyl and the amide were replaced by hydrogens. However, a semiempirical study on **2b** indicated that if calculations include increasing ribose-like bulk, the rotational profile of the glycosylic bond changes, resulting in shifted minima and increased barrier heights.

Not only are some of the populations obtained for **2a**−**5a** probably overestimated but the electrostatic interactions in high dielectric media *(ie.* physiological conditions) are expected to give much smaller free energy contribution than *in vacuo.* Thus, the energy profiles around the glycosylic bond presented in previous papers are likely to be biased by a large electrostatic term and the lack of van der Waals interactions due to the omitted ribose moiety (in case of **2a** and **4a)** and the lower levels of theory applied.

Ab Initio Computations

Full geometry optimization of **2b** and **4b** at the 3-21G* level followed by a single point calculation at the 6-31G* level confirmed the previous results regarding the large charge separations by the NBO method.[10] The more reliable electrostatic charges,[11] however, show a slight negative charge on the S and a smaller negative charge on the oxygen (Table 1). Incorporation of the d orbitals (6-31G*) gives rise to a drop in the point charges compared to lower levels, which is in accord with tendency discovered for thiophenes.[12] In addition, we also noticed the presence of an intramolecular hydrogen bond between C2′−OH and N3 in case of tiazofurin (d_{N-O} = 2.526 Å) which was not observed for the oxazole derivative (d_{N-O} = 4.003 Å). This difference, which apparently could not be seen using model fragments, was also detected at the MNDO level.

Stationary point calculations on **2b**−**5b** were carried out with 20° increments at the 3-21G*/6-31G* level. The energy profiles are depicted in Figure 2a,b. The 2′-endo sugar pucker uniformly allows lower energy minima than the 3′-endo ring as it was found in the solid state as well.[3,4,6,7] This is simply due to the larger vdW violations in the 3′-endo conformations (Table 2). To assess the steric influence imposed by C2′-H, the energy barriers of model fragments (ribose replaced by a CH_3OCH_2 group fixed in a ribose-like orientation, **2c**−**5c**, respectively) were computed. It is clear from the data (Figure 2a−c) that, even *in vacuo,* about half of the humps in energy of the S-nucleosides is accounted for by the interaction of C2′-H with S1. There is only a slight change in case of the O-nucleosides in the lack of vdW violation at 120° for these molecules (Table 2).

NBO analysis is frequently used to estimate stabilization derived from charge transfer and delocalization.[10] Second-order perturbation analysis of the Fock matrix failed to pinpoint a single source of the above effects at $\phi = 0°$. This conformation of **2b** is stabilized by a $\sigma-\sigma^*$ charge transfer centered on O4′−C1′ and C2−N3 bonds, respectively. However, similar stabilization of the same magnitude centered on O4′−C1′ and C2−S1 bonds was found in anti ($\phi = 180°$) conformation as well. Deletion of all Rydberg and antibond orbitals removes all charge transfer delocalizations; thus the overall contribution of those effects can be calculated. The syn conformation was shown to be stabilized (**2b**, 6.1; **3b**, 9.3; **4b**, 5.0; **5b**, 1.76 kcal/mol) compared to the trans orientation in all cases. This fact in conjunction with the lack of correlation with the observed energy differences between the two states indicate that other interaction types such as electrostatic interaction (attractive or repulsive) or exchange repulsion (vdW violation, repulsive) may have a prominent influence on the potential surface of this class of molecules.

Semiempirical Solvation Model

The COSMO solvation model[13] with the MNDO parameter set was applied to approximate the effect of high dielectric media. MNDO was previously found to give the best consistency with the *ab initio* results.[5] The energy profile was found essentially the same for both 2′-exo and 2′-endo puckered rings because the ribose pucker is negligibly small at the MNDO semiempirical level. The calculations on the model fragments (*i e.* the ribose replaced by CH_3OCH_2, **2c**−**5c**) reveal that exposure of all polar heteroatoms to solvent would be favored in the lack of the steric effect of C2′-H (Figure 3b). This would maximize the solvation free energy. The energy profiles of the full molecules (Figure 3a), however, show curves having deep minima around 40° and 140°, values where there is no interference with C2′-H. The minima are shifted with respect to the *ab initio* wells to provide the largest possible exposure to solvent. The data for **5b** imply that the semiempirical model seems to underestimate the O4′−O1 repulsion at $\phi = 0°$.

Molecular Dynamics Simulations

Molecular dynamics (MD) techniques are particularly useful to investigate free energy differences among a pool of conformations if the Boltzmann equilibrium is established. A combined Monte Carlo/MD method implemented in Macromodel[14] has been devised to increase the efficiency of sampling. Unfortunately, the MM2 and MM3 force fields included in the package lack many high-quality parameters for **2b**−**5b**. Therefore we used the Tripos force field of Sybyl which has been shown to be a good general force field for organic molecules.[15] The 1 ns pure MD runs *in vacuo* were carried out at 400 K in order to increase the crossing of high-energy barriers. In a separate series of simulations, the dielectric constant was set to 78 to study the influence of a polar environment. This technique can provide clues of the conformational behavior in solvent for small molecules that do not bury significant surface areas. Although these lengthy calculations should be robust enough to explore essentially one rotatable bond in the molecules, one has to bear in mind that the results can only be approximate. The charge distribu-

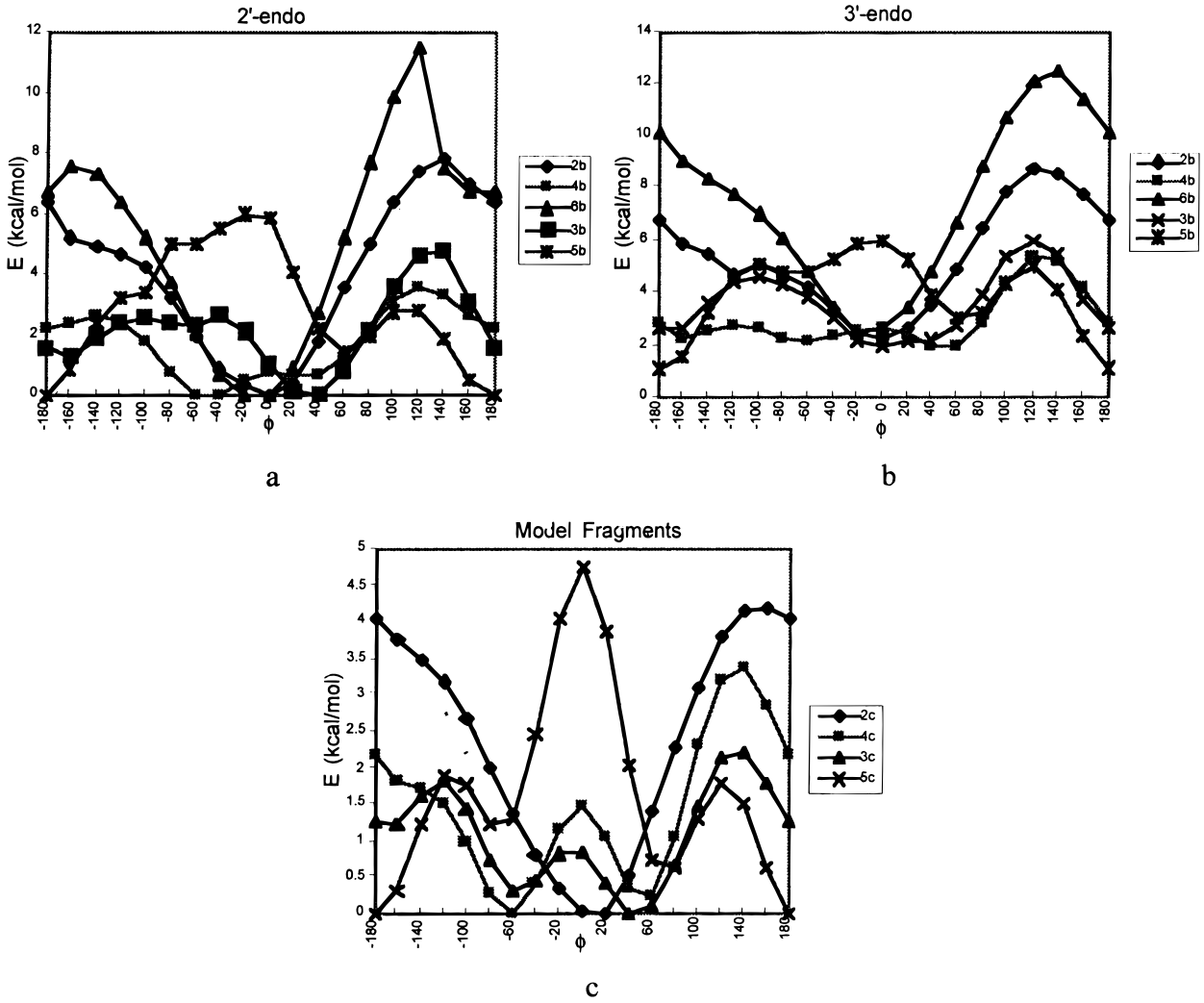

Figure 2. *Ab initio* energy profiles around the glycosylic angle.

Table 2. Atom Distances (Å) at Various Conformations[a]

glycosylic angle	**2b**		**3b**		**4b**		**5b**	
(atom pairs)[b]	2′-endo	3′-endo	2′-endo	3′-endo	2′-endo	3′-endo	2′-endo	3′-endo
0° (O4′−X1)	**2.877**	**2.797**	**2.796**	**2.770**	2.766	**2.683**	**2.701**	**2.648**
120°(H2′−X1)	2.838	**2.722**	2.850	**2.725**	2.509	**2.383**	2.509	**2.383**
180°(O4′−X3)	**2.769**	**2.725**	**2.771**	**2.750**	2.915	**2.844**	2.906	**2.857**

[a] Distances within the sum of vdW radii are highlighted. [b] **2b**, Xl = S1, X3 = N3; **3b**, X1 = S1, X3 = C3; **4b**, X1 = O1, X3 = N3; **5b**, X1 = O1, X3 = C3.

tion in the heterocyclic rings fluctuate due to electrostatic interaction of the π system with the ribose oxygen (polarization). For instance, O1 in oxazofurin is less negative in the syn orientation than when it faces away from the ribose. We could only apply a constant set of charges for the MD runs; therefore small deviations from the populations presented on Figures 4 and 5 are expected. The MD results also imply that the repulsion of the oxygens at syn conformation might have been underestimated by the MNDO method especially for furanfurin. Besides that, there is a significant qualitative agreement with the *ab initio* and semiempirical calculations. We also evaluated the flexibility of the glycosylic dihedral angle based on the MD results using a simplified modification of Karplus' technique to quantify conformational entropy.[16] A larger number for the flexibility factor (*f*) which is independent on the energy profile means more rigidity for a given angle. Table 3 confirms that oxazofurin is more flexible than tiazofurin both *in vacuo* and in solvent which is in accord with the observation of several conformations for the former in a single crystal by X-ray crystallography. All molecules show higher flexibility in solvent (Table 3) as the contribution of intramolecular electrostatic effects become diminished due to interaction with the polar environment.

Discussion

All *ab initio* calculations that have been carried out on thiophene-like systems indicate that the actual electron deficiency on the sulfur is quite small (or S might slightly be negative) and is greatly dependent on the basis set.[12] The positive charge decreases in general with inclusion of d, f orbitals and electron correlation. Thus, calculations of the energy profiles of **2**−**5** at lower *ab initio* levels are biased by an overestimated electrostatic term. The energy barriers for **2b**−**6b** at 3-21G* were 2−3 kcal/mol higher than those at 6-31G* (data not shown). This trend is expected to hold at even higher levels of theory. In addition, the electrostatic

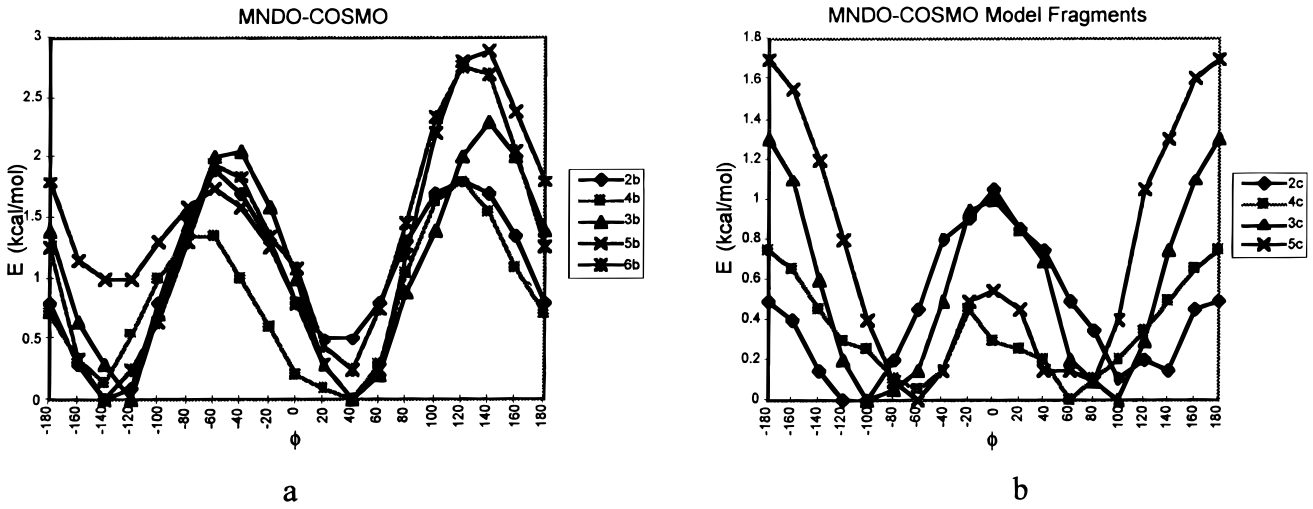

Figure 3. Semiempirical solvation energy profiles around the glycosylic angle.

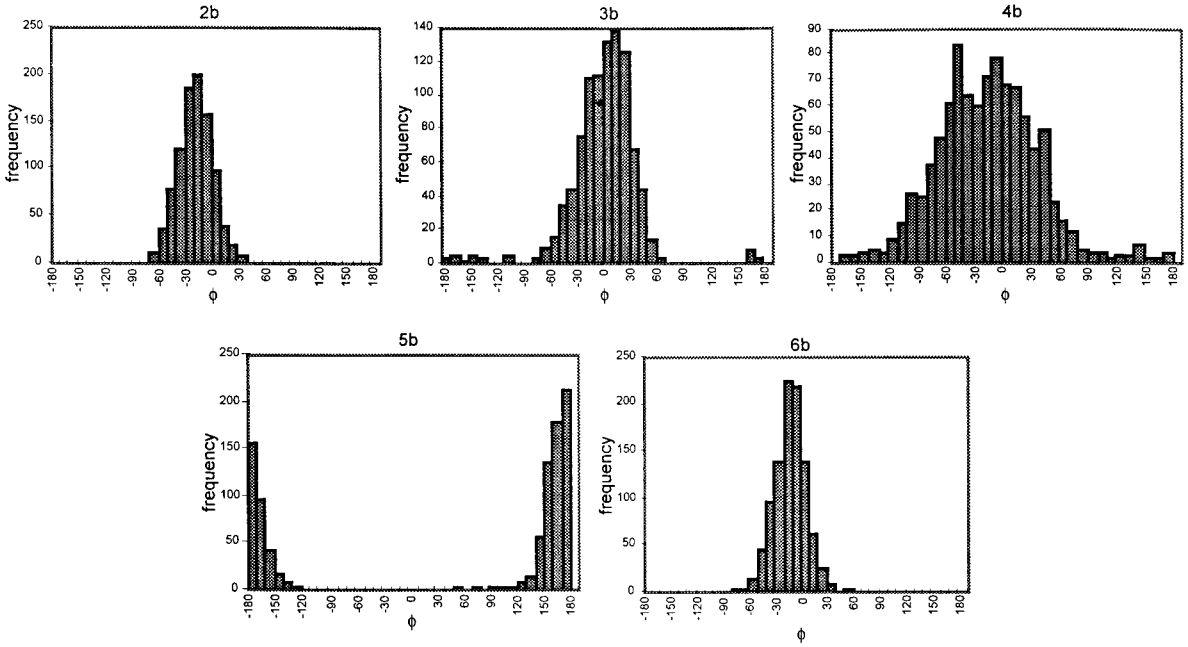

Figure 4. Conformational populations of **2b**−**6b** *in vacuo.*

effects become less important in high dielectric media such as physiological conditions. The steric effects are, on the other hand, not influenced by the polarity of the surrounding media.

Our calculations, which are mostly consistent with the large body of experimental data available, suggest that the ribose moiety plays a decisive role in the conformational equilibrium around the glycosylic torsional angle. Therefore it cannot be neglected in such calculations. The energy minimum in thiophenfurin occurs at a higher angle value than that in tiazofurin. The location of the energy wells is rather determined by exclusion of unfavorable structures due to vdW violations than by a driving force due to favorable S−O interaction (Table 2, NBO analysis). Charge transfer and presumably polarization interaction contribute to stabilization of the S-nucleosides at $\phi = 0°$ which may be the reason behind the observation of numerous close S−O contacts in crystallographic databases.[5]

All calculations confirm that conformational properties of furanfurin are unique leading to an inactive analogue. There is only a slight hump in *ab initio* energy for oxazofurin at $\phi = 0°$, and the local minimum at −50° is somewhat deeper than that between 10° and 60°. However, solvation clearly seems to favor the positive region over the negative. These effects jointly may lead to the observed values in the X-ray structures of **4a**. Oxazofurin is more flexible than the S-nucleosides. Although the minimum-energy conformation of oxazofurin may not coincide with that of tiazofurin, the latter is certainly accessible for **4a** due to its large flexibility. The estimated rotational barrier of **4a** is in the range of that of ethane. Thus, the loss in binding energy for **4a** in order to adopt a tiazofurin-like conformation in the active site of the target enzyme is not likely to be significant enough to explain the difference of several orders of magnitude in IC_{50} values. Alternatively, the negative oxygen of **4a** could interfere with an active site residue of either IMPD or a kinase that would stabilize NAD^+, **2a**, and **3a** due to favorable electrostatic contacts.

The conversion of **5a** to the active dinucleotide has been shown to take place only with 10% efficiency compared to **3a**.[3] This phosphorylating enzyme may

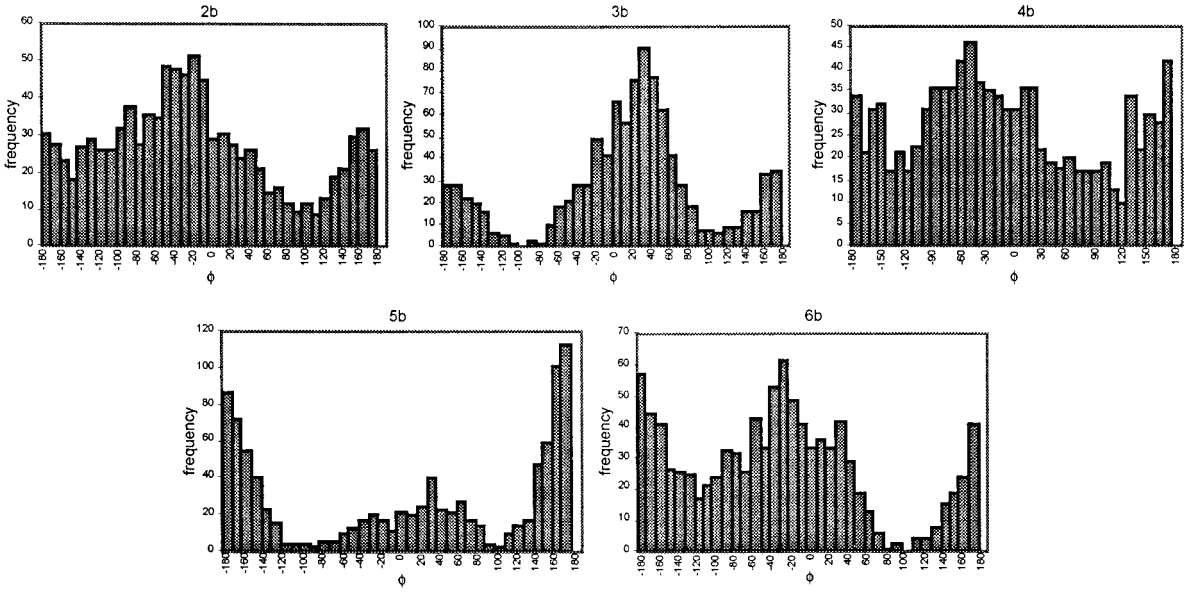

Figure 5. Conformational populations of **2b**−**6b** in water model.

Table 3. Flexibility of **2b**−**6b**

f	**2b**	**3b**	**4b**	**5b**	**6b**
$D = 1$	5.57	4.39	2.77	5.63	5.98
$D = 78$	1.11	2.38	0.92	2.80	1.64

well be nicotinamide ribonuclease kinase that has recently been shown to convert tiazofurin to TAD.[17] The apparent K_m for **2a** was 1 order of magnitude higher than that for nicotinamide ribonucleoside. The latter bears a significant positive charge at the nicotinamide region. Thus, it is not impossible that the negative oxygen is responsible for the low activity of oxazofurin and furanfurin via inhibition of binding to the kinase that converts the active analogues to the dinucleotide form. This notion, originally proposed by Goldstein *et al.*, now gains further support by the data reported herein.

Conclusions

Our calculations suggest that most of the conformational properties of tiazofurin analogues could be explained solely based on steric interactions. Therefore any moiety replacing the sulfur of tiazofurin needs to be large enough to impose a significant rotational barrier around the glycosylic bond and of positive character or alternatively hydrogen bond donor. Such an analogue could be **6a** that exhibits an almost identical behavior to **2a** in our calculations (Figures 2−5, Table 3). The techniques applied in this report enable the rational design of new derivatives with a potential for improved activity and decreased toxicity.

Experimental Section

The *ab initio* point charge calculations were carried out with the Gaussian 94 program[18] on an SGI R4500 Indy workstation. All geometries were fully optimized using the standard HF/3-21G* basis set. Charge distributions were calculated at HF/3-21G*, HF/6-31G* levels utilizing the natural bond orbital (NBO) analysis as implemented in Gaussian 94.[10] Electrostatic potential derived atomic charges were obtained by the CHelpG scheme available in the package. The GAMESS package[19] was used for the stationary point calculations at the HF/3-21G*/6-31G* level on SGI R10000 workstations. The ϕ torsional angle was fixed at each point (20° increments) while the rest of the **z**-matrix elements were optimized. NBO analyses were done on a Cyrix 166+ PC computer with the NBO 3.0 program linked to PC GAMESS.[19]

The semiempirical calculations were carried out with Mopac93 (QCPE no. 455) using the COSMO solvation model (keywords: NSPA = 60 EPS = 78.4 GNORM = 0.5). The torsional angles were altered in 20° increments for two full cycles and the average values of the heat of formations for each angle were used in figures.

Molecular dynamics simulations were run for 1 ns at 400 K (1.5 fs time steps, 0.1 ps coupling factor) with the Tripos force field implemented in SYBYL 6.2.[20] Dielectric constant was set to 1 (*in vacuo*) and 78 (water model), respectively. Boltzmann initial velocities were used to equilibrate the systems for 50 ps before data collection. Energy minima from MNDO/COSMO calculations were applied as starting structures with the corresponding MOPAC/COSMO charges. The torsional angles were measured with SYBYL's spreadsheet.

The flexibility values (*f*) were calculated as follows. The torsional angle values were classified into 36 intervals (10° increment). The standard deviation of the relative frequencies was calculated and multiplied by 100 to give *f*.

Acknowledgment. G.M.M. thanks Dr. G. R. Marshall and J. W. Ponder for the helpful discussions.

References

(1) (a) Cooney, D. A.; Jayaram, H. N.; Gebeyehu, G.; Betts, C. R.; Kelley, J. A.; Marquez, V. E.; Johns, D. G. The Conversion of 2-β-D-Ribofuranosyl-thiazole-4-carboxamide to an Analogue of NAD with Potent IMP Dehydrogenase-inhibitory Properties. *Biochem. Pharmacol.* **1982**, *31*, 2133−2136. (b) Kuttan, R.; Robins, R. K.; Saunders, P. P. Inhibition of Inosinate Dehydrogenase by Metabolites of 2-β-D-Ribofuranosylthiazole-4-carboxamide. *Biochem. Biophys. Res. Commun.* **1982**, *107*, 862−868.

(2) Goldstein, B. M.; Bell, J. E.; Marquez, V. E. Dehydrogenase Binding by Tiazofurin Anabolites. *J. Med. Chem.* **1990**, *33*, 1123−1127.

(3) Franchetti, P.; Cappellacci, L.; Grifantini, M.; Barzi, A.; Nocentini, G.; Yang, H.; O'Connor, A.; Jayaram, H. N.; Carrel, C.; Goldstein, B. M. Furanfurin and Thiophenfurin: Two Novel Tiazofurin Analogues. Synthesis, Structure, Antitumor Activity, and Interactions with Inosine Monophosphate Dehydrogenase. *J. Med. Chem.* **1995**, *38*, 3829−3837.

(4) Goldstein, B. M.; Li, H.; Hallows, W. H.; Langs, D. A.; Franchetti, P.; Cappellacci, L.; Grifantini, M. C-Glycosyl Bond Conformation in Oxazofurin: Crystalographic and Computational Studies of the Oxazole Analogue of Tiazofurin. *J. Med. Chem.* **1994**, 37, 1684−1688.

(5) Goldstein, B. M.; Burling, F. T. Computational Studies of Nonbonded Sulfur-Oxygen and Selenium-Oxygen Interactions in the Thiazole and Selenazole Nucleosides. *J. Am. Chem. Soc.* **1992,** *114,* 2313−2320.

(6) Li, H.; Hallows, W. H.; Punzi, J. S.; Marquez, V. E.; Carrell, H. L.; Pankiewicz, K. W.; Watanabe, K. A.; Goldstein, B. M. Crystallographic Studies of Two Alcohol Dehydrogenase-Bound Analogues of Thiazole-4-carboxamide Adenine Nucleotide (TAD), the Active Anabolite of the Antitumor Agent Tiazofurin. *Biochemistry* **1994**, *33*, 23−32.
(7) Goldstein, B. M.; Takusagawa, F.; Berman, H. M.; Srivastava, P. C.; Robins, R. K. Structural Studies of a New Antitumor Agent: Tiazofurin and Its Inactive Analogues. *J. Am. Chem. Soc.* **1983,** *105*, 7416−7422.
(8) Sintchak, M. D.; Fleming, M. A.; Futer, O.; Raybuck, S. A.; Chambers, S. P.; Caron, P. R.; Murcko, M. A.; Wilson, K. P. Structure and Mechanism of Inosine Monophosphate Dehydrogenase in Complex with the Immunosuppressant Mycophenolic Acid. *Cell* **1996**, *85*, 921−930.
(9) Hedstrom, L.; Wang, C. C. Mycophenolic Acid and Thiazole Adenine Dinucleotide Inhibition of *Tritrichomonas foetus* Inosine Monophosphate Dehydrogenase: Implications on Enzyme Binding. *Biochemistry* **1990,** *29*, 849−854.
(10) Reed, A. E.; Curtis, L. A.; Weinhold, F. Intramolecular Interactions from a Natural Bond Orbital, Donor-Acceptor Viewpoint. *Chem. Rev.* **1988**, *88*, 899−926.
(11) (a) Breneman, C. M.; Wiberg, K. B. Determining Atom-Centered Monopoles from Molecular Electrostatic Potentials. The Need for High Sampling Density in Formamide Conformational Analysis. *J. Comput. Chem.* **1990**, *11*, 361−373. (b) Tsuzuki, S.; Uchimann, T.; Tanabe, K.; Yliniemala, A. Comparison of Atomic Charge Distributions Obtained from Different Procedures-Basis Set and Electron Correlation Effects. *J. Mol. Struct. THEOCHEM* **1996**, *365*, 81−88.
(12) Henriksson-Enflo, A. Theoretical Calculations on Thiophenes. In *Thiophene and its Derivatives;* Gronowitz, S., Ed.; Wiley: New York, 1985; pp 215−259.
(13) Klamt A.; Schurmann, G. COSMO: A New Approach to Dielectric Screening in Solvents with Explicit Expressions for the Screening Energy and its Gradient. *J. Chem. Soc., Perkin Trans. 2* **1993**, 799−805.
(14) MacroModel 5.5, Department of Chemistry, Columbia University, New York, NY 10027.
(15) Clark, M.; Cramer, R. D., III; Opdenbosch, N. V. Validation of the General Purpose Tripos 5.2 Force Field. *J. Comput. Chem.* **1989**, *10*, 982−1012.
(16) Karplus, M.; Kushick, J. N. Method for Estimating the Configurational Entropy of Macromolecules. *Macromolecules* **1981**, *14*, 325−332.
(17) Sasiak, K.; Saunders, P. P. Purification and Properties of a Human Nicotinamide Ribonucleoside Kinase. *Arch. Biochem. Biophys.* **1996**, *333*, 414−418.
(18) Gaussian 94, Revision B.2, Frisch, M. J.; Trucks, G. W.; Schlegel, H. B.; Gill, P. M. W.; Johnson, B. G.; Robb, M. A.; Cheeseman, J. R.; Keith, T.; Petersson, G. A.; Montgomery, J. A.; Raghavachari, K.; Al-Laham, M. A.; Zakrzewski, V. G.; Ortiz, J. V.; Foresman, J. B.; Cioslowski, J.; Stefanov, B. B.; Nanayakkara, A.; Challacombe, M.; Peng, C. J.; Ayala, P. Y.; Chen, W.; Wong, M. W.; Andres, J. L.; Replogle, E. S.; Gomperts, R.; Martin, R. L.; Fox, D. J.; Binkley, J. S.; Defrees, D. J.; Baker, J.; Stewart, J. P.; Head-Gordon, M.; Gonzalez, C.; Pople, J. A., Gaussian, Inc., Pittsburgh, PA, 1995.
(19) GAMESS version 22 Nov 1995 and PC GAMESS 4.0; Schmidt, M. W.; Baldridge, K. K.; Boatz, J. A.; Elbert, S. T.; Gordon, M. S.; Jensen, J. H.; Koseki, S.; Matsunaga, N.; Nguyen, K. A.; Su, S. J.; Windus, T. L.; Dupius, M.; Montgomery, J. A., Iowa State University, General Atomic and Molecular Electronic Structure System. *J. Comput. Chem.* **1993,** *14*, 1347−1363.
(20) Tripos, Inc., 1699 S Hanley Rd, St. Louis, MO 63144-2913.

JM970129S